Ultrathin Ferroelectric P(VDF/TrFE) Copolymer Film in Low-Cost Non-Volatile Data Storage Applications

*Jong Soon Lee, A. Anand Prabu, You Min Chang, Kap Jin Kim**

Summary: Ultrathin ferroelectric P(VDF/TrFE(72/28) films were used in the fabrication of metal-ferroelectric polymer-metal single bit device with special emphasis on the formation of uniform film surface, faster dipole switching time under an external electric field, and longer memory retention time. FTIR-GIRAS and AFM were used complementarily in analyzing the changes in chain orientation and surface crystalline morphology with varying sample preparation methods. It was found that the magnitudes of remnant polarization and coercive field are highly related to the degree of chain orientation along the conductive substrate surface. The cast-annealed sample showed the highest polarization and the smallest coercive field. DC-EFM technique was successfully used to 'write and erase' the data bit on the ultrathin P(VDF/TrFE) film by applying a dc bias voltage much larger than coercive voltage with different polarities and the data bit state could be read by measuring the piezoelectric response of the cantilever with a lock-in amplifier by applying an ac modulating voltage whose V_{pp} is much less than the coercive voltage.

Keywords: atomic force microscopy; ferroelectricity; FTIR-GIRAS; P(VDF/TrFE); P-E hysteresis

Introduction

Non-volatile ferroelectric polymer random access memory (NV-FePoRAM) devices based on ferroelectric polymers have the potential to overcome many of the fabrication issues faced in the inorganic semiconductor industry.[1] Advanced local probing technique in scanning probe microscopy (SPM) has led many researchers to propose SPM-based ultrahigh density data storage devices using scanning tunneling microscope (STM), atomic force microscope (AFM), electrostatic force microscope (EFM), scanning capacitance microscope (SCM), magnetic force microscope (MFM), and scanning near-field optical microscope (SNOM).[2–5] More recently, IBM and LG have demonstrated a low power SPM probe-based high density data storage system using a new read-write mechanism called ''Thermo-piezoelectric method'' in which the cantilever tip equipped with a heater is used for making an indentation (stands for a logical '1') on a PMMA film.[6,7] However, the main drawback is that writing data by this thermal method changes the polymer surface morphology and limits its usage to Write-Once-Read-Many (WORM) applications. Also, high electric power consumption for heating the AFM tip above 300 °C is another considerable issue. Replacing PMMA with ferroelectric ultrathin poly(vinylidene fluoride-trifluoroethylene) (P(VDF/TrFE)) copolymer films is of even greater interest in the fabrication of NV-FePoRAM for Write-Many-Read-Many (WMRM) applications as well as resolve the high power consumption problem.

Nonvolatile data writing capability of P(VDF/TrFE) is performed by electrically switching the C-F dipole under external electric field about two times larger than

Department of Advanced Polymer and Fiber Materials, Kyung Hee University, Yongin, Gyeonggi-do 446-701 Korea
Fax: (+82) 31 2012518
E-mail: kjkim@khu.ac.kr

coercive field (when $E > 2E_c$, '1' state and when $E < -2E_c$, '0' state). Due to bi-stable polarization-electric field behavior (P-E hysteresis), once switched dipole does not change its polarization, resulting in positive or negative remnant polarization ($\pm P_r$) depending on the dipole direction even after removing the external electric field.[8] As the magnitude of P_r is larger, the piezoelectric response signal is also larger when we apply an ac modulating voltage, whose peak value is smaller than coercive voltage, to non-destructively read the data bit. P_r in thin films is mainly dependent on the crystallinity and the degree of chain and dipole orientation, which in turn is highly dependent on film preparation methods.[9–12] Therefore it is very important to prepare ultrathin P(VDF/TrFE) film with uniform film thickness and the highest possible P_r in the fabrication of SPM-based storage or FeRAM devices.

In this paper, we investigate the effect of sample preparation methods on the surface morphology, chain and dipole orientation, ferroelectric and NV-memory characteristics using FTIR-GIRAS, AFM, DC-EFM, and P-E hysteresis methods to study the feasibility of using ultrathin P(VDF/TrFE) films in SPM-based data storage or NV-FePoRAM devices.

Experimental Part

P(VDF/TrFE) (72/28 mole%) samples in the form of pellets have been obtained from Solvay, USA. The P(VDF/TrFE) ultrathin films were prepared as follows. 50, 100, and 200 nm thick films were prepared by spin casting different wt% of P(VDF/TrFE) in MEK solvent with a spin-coater (1500 rpm for 30 s) under N_2 atmosphere on the gold-coated glass and ITO glass. All the films were processed under different thermal conditions (a) as cast (AC) at R.T., (b) as cast-annealed (AN) above Curie transition temperature, but below the melting temperature (120 °C, 3 h), (c) melt (200 °C, 10 min)-quenched (MQ), and (d) melt (200 °C, 10 min)-slowly cooled (−2 °C/min) (MSC). The average thickness of the films cast on ITO substrate was measured using an atomic force microscope (XE-100, PSIA, Korea) at room temperature. The film surface morphology was characterized with the same AFM at non-contact mode. FTIR-GIRAS (grazing incident reflection absorption spectroscopy) data for samples cast on gold-coated glass were collected using Bruker-IFS66V spectrometer (300 scans, incidence angle ca. 85° from the normal to the surface and 2 cm^{-1} resolution). For electrical measurements, Al electrodes of 200 μm dia. were vacuum-deposited on the top surface of the cast films on ITO glass. P-E hysteresis curves were obtained using a ferroelectric tester (Precision LC, Radiant Technologies, USA). The piezoelectric response images of AN films were obtained using XE-100 (PSIA, Korea) using a cantilever with a Ti-Pt coated tip in the dynamic contact EFM mode (DC-EFM).

Results and Discussion

Changes in Crystallinity, Chain and Dipole Orientation

As shown in Figure 1(a), the unit cell of β-crystal phase in P(VDF/TrFE) is orthorhombic, CF_2 dipoles parallel to *b*-axis, and molecular chain along the *c*-axis.[13] We have already reported the sensitivity of FTIR-GIRAS to changes in crystallinity, chain and dipole orientation in ultrathin films.[14,15] In GIRAS used without a polarizer with the IR incident angle closer to grazing incident angle (ca. $80 \sim 88°$), it predominantly detects the vibrational modes with the transition moments normal to the substrate surface (Figure 1(b)).

Figure 2 exhibits the FTIR-GIRAS spectra showing changes in chain orientation and crystallinity for 50 and 100 nm thick P(VDF/TrFE) films prepared under varying thermal conditions. Compared to the AC samples, the characteristic bands of *trans*-zigzag conformation of the AN samples, e.g. the 1289 cm^{-1} band (A_1, $\vec{\mu} \parallel \vec{b}$) for

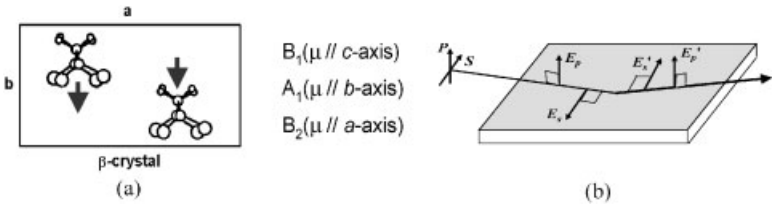

Figure 1.
(a) Unit cell of β-crystal phase of P(VDF/TrFE). Arrows represent CF_2 dipole moments. $\vec{\mu}$ is vibrational transition moment of each symmetry group; (b) Fundamental concept of GIRAS: After reflection at around grazing angle, vibrational band intensities parallel to *s*-polarization are cancelled out and those parallel to *p*-polarization are enhanced.

the VDF *trans* sequence longer than TTTT, the 848 cm^{-1} band (A_1, $\vec{\mu} \parallel \vec{b}$) for the *trans* sequence longer than TTT, and 1182 and 884 cm^{-1} bands (B_2, $\vec{\mu} \parallel \vec{a}$) associated with crystalline phase show increase in the absorption intensity due to increased crystallinity after annealing.

For AC and AN samples, the intensity of 1402 cm^{-1} band (B_1, $\vec{\mu} \parallel \vec{c}$), whose transition moment is along the chain direction, is comparatively weaker than that observed for MQ and MSC samples. This indicates that the molecular chains are preferentially oriented along the radial direction of the substrate in the course of spin-casting process and not allowing any relaxation from chain extended state to random coiled state.

Compared to AC sample, reduced intensity of 1402 cm^{-1} in AN sample is attributed to the fact that some random coiled chains present even after spin-casting undergoes thermal relaxation resulting in preferential orientation of *trans*-zigzag chains parallel to the substrate surface with the dipoles parallel along the poling direction during annealing.[16]

From GIRAS data, AC-AN method was found to be most suitable for preparing samples with maximum dipole orientation along the poling direction. For MQ and MSC samples, there are some changes in

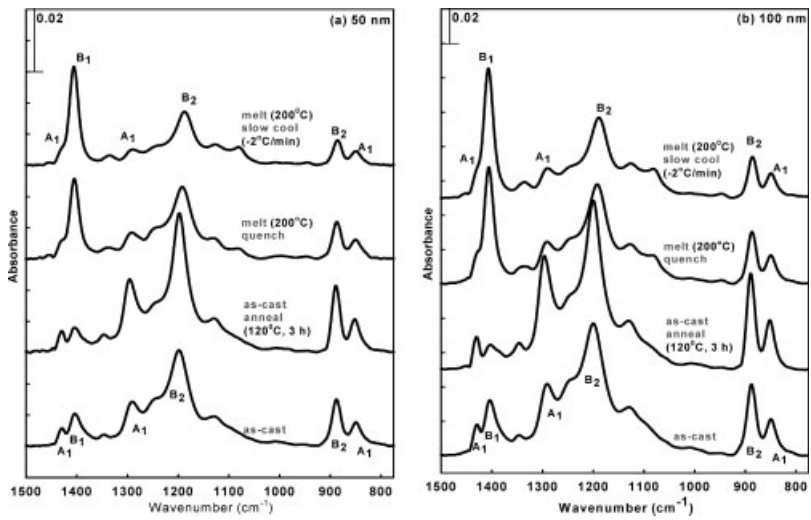

Figure 2.
FTIR-GIRAS spectra measured at room temperature for 50 and 100 nm thick P(VDF/TrFE) films obtained with different preparation methods.

chain orientation along the normal to the surface plane resulting in an increase in B_1 band intensity. With the preferential chain orientation for the MQ and MSC samples parallel to the poling direction, it is almost impossible for the C-F dipoles to switch along the poling direction and hence unsuitable for device fabrication.

Surface Topography

We can predict orientation pattern of lamellar crystal on the surface of ITO or gold substrate from FTIR-GIRAS results of the P(VDF/TrFE) ultrathin films prepared with different sample preparation methods. Since molecular chains are preferentially oriented along the substrate surface for the AC and AN samples, the chain-folded lamellar crystals are predicted to be arranged with edge-on type predominantly as shown in Figure 3(a). On the contrary, face-on lamella crystalline domains for the MQ and MSC samples are predicted predominantly as shown in Figure 3(b), since molecular chains are preferentially oriented normal to the substrate surface.

50 nm thick P(VDF/TrFE) films were subjected to different thermal conditions and their AFM images and histograms are shown in Figure 4. Our emphasis is to prepare the flattest possible surface with minimum deviation in film thickness in order to avoid the electrical breakdown. AC and AN samples shown in Figure 4(a) and (b) exhibit very tiny edge-on crystalline micro-domains with short needle like shape, whose average length and width are approximately 110 and 30 nm, respectively, as shown in the inset. These two samples also show relatively uniform film thickness as evidenced from their respective histograms.

MQ and MSC samples shown in Figure 4(c) and (d) exhibit drastically changed surface morphology with non-uniform film thickness during non-isothermal crystallization from the melt. The MQ and MSC samples are seen to have predominantly face-on lamella crystalline domains as predicted from FTIR-GIRAS results and also consistent with our previous report.[16] The MQ sample also has a small amount of a long edge-on lamellar crystal, whose thickness and height are about 140 and 25 nm, respectively, as shown in inset. When considering the average lamella thickness of common crystalline polymer to be 10~12.5 nm, this edge-on lamellar crystal domain consists of a stack of about 12 lamellae. The average thickness of

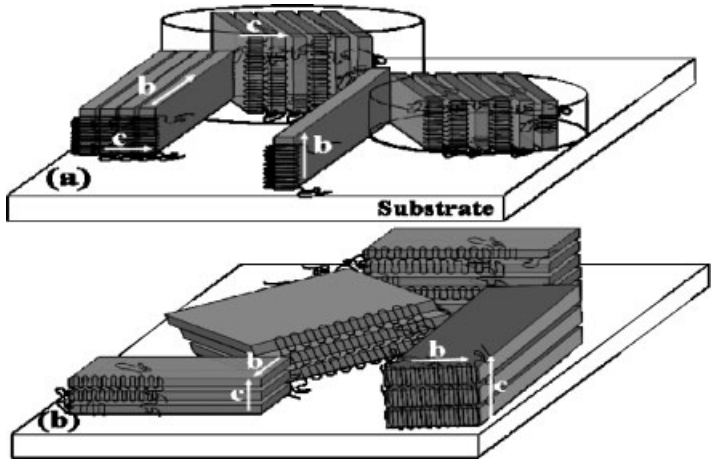

Figure 3.
A schematic of microstructure predicted from FTIR-GIRAS data. (a) edge-on lamellar crystal and (b) face-on lamellar crystal.

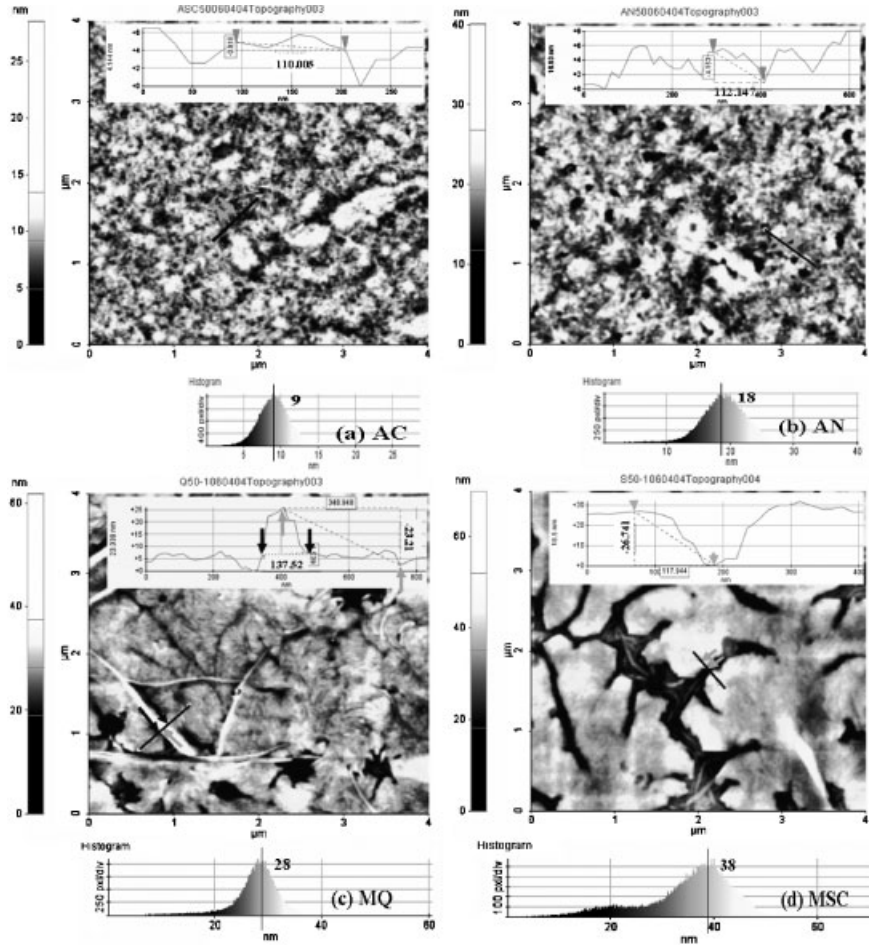

Figure 4.
AFM 2D-topography image (NC mode) of P(VDF/TrFE)(72/28) 50 nm thick film as a function of sample preparation condition. Scanned area is 4 μm × 4 μm.

face-on lamellar crystals in Figure 4(d) are found to be about 25 nm (see inset), which indicates that this face-on lamellar crystal consists of a stack of two lamellae. The surface topography of 100 and 200 nm thick samples (not shown here) is also nearly same as that of 50 nm thick sample for the AC and AN samples, whereas more edge-on lamellar crystals are observed on the face-on lamellae with increasing film thickness for MQ and MSC samples. It is very interesting that the surface morphology of each sample prepared with different sample preparation methods is very consistent with the surface topography predicted from our FTIR-GIRAS data.

P-E Hysteresis

Though AC and AN samples exhibit preferential molecular chain orientation (c-axis) along the substrate surface, both *a*- and *b*-axes can rotate around the *c*-axis randomly. The external electric field applied in P-E measurement induces the preferential orientation of the polar *b*-axis along the electric field direction leading to large and permanent polarization of C-F dipoles. For MQ and MSC samples, since

most of *c*-axes are normal to the substrate surface, i.e., parallel to the external electric field, it is impossible to get the preferential orientation of the polar *b*-axis towards the electric field direction.

For the 50 nm thick samples, P-E hysteresis loops could not be obtained at all due to the low crystallinity and frequent electric breakdown caused by pin-hole defects. Figure 5 shows P-E hysteresis loops of 100 nm films prepared at various thermal conditions. Most of P-E curves show asymmetric hysteresis, which may be caused by the difference in chemical composition between top (aluminum) and bottom (ITO) electrodes. So, the remnant polarization (P_r) and coercive electric field (E_c) are obtained from the average of $\pm P_r$ and $\pm E_c$, respectively. For AN sample (see Figure 5(a)), P_r and E_c are approximately 7.1 $\mu C/cm^2$ and 0.68 MV/cm, respectively, when the applied electric field is at 1.5 MV/cm. For the MQ and MSC samples (see Figure 5(b) and (c)), P_r is reduced considerably and E_c is dramatically increased at the same external electric field strength of 1.5 MV/cm. The reduction in P_r is associated with the reduced amount of edge-on lamellar crystals and the abrupt increase in E_c is associated with the increased amount of face-on lamellar crystals.

Piezoelectric Response Using DC-EFM

The detection of the poled areas was carried out by measuring the piezoelectric response in the DC-EFM mode on the XE-100 AFM. An ac modulating voltage between the probe tip and the conductive substrate induces the mechanical oscillation normal to the film surface in the poled areas, because P(VDF/TrFE) is a piezoelectric material. The amplitude of the ac modulating voltage must be far below the coercive voltage in order not to change the initial polarization direction while reading data written once. This piezoelectric vibration amplitude is proportional to the modulating voltage and P_r, and thus the piezoresponse signal is measured from the cantilever deflection using a lock-in-amplifier. The detected signal is comprised of the amplitude (A) and the phase difference (ϕ), which correspond to the magnitude and the direction of the polarization in the film, respectively. In this study, $A\cos\phi$ images with which both magnitude and direction of polarization can be evaluated simultaneously and phase difference images with which the direction of polarization can be only identified were obtained. The frequency and magnitude of the ac modulating peak-peak voltage used for reading a data bit were 17 kHz and 2 V.

Figure 6 shows topographic and piezoresponse images of 200 nm thick AN film obtained simultaneously. Figure 6(a) shows the topographic image after poling the film in an area of 4×4 μm^2 with a dc bias voltage of +20V for a duration of 0.5 sec per data bit. We cannot observe the poled area with a certain level of contrast in a simple topographic image, but observe small

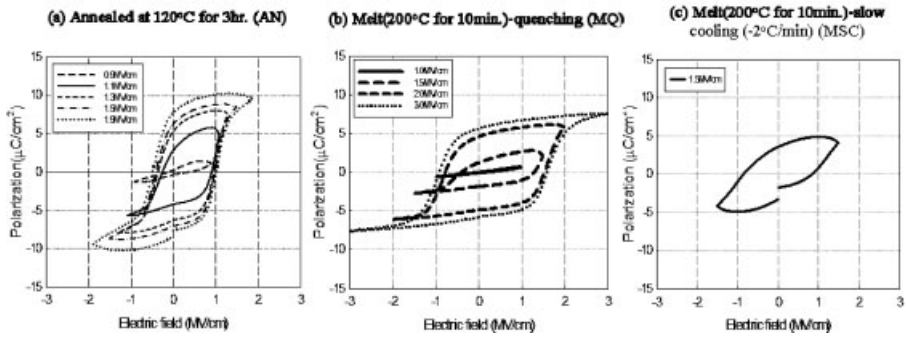

Figure 5.
Changes in the P-E hysteresis loop with various thermal treatments for 100 nm thick P(VDF/TrFE) film.

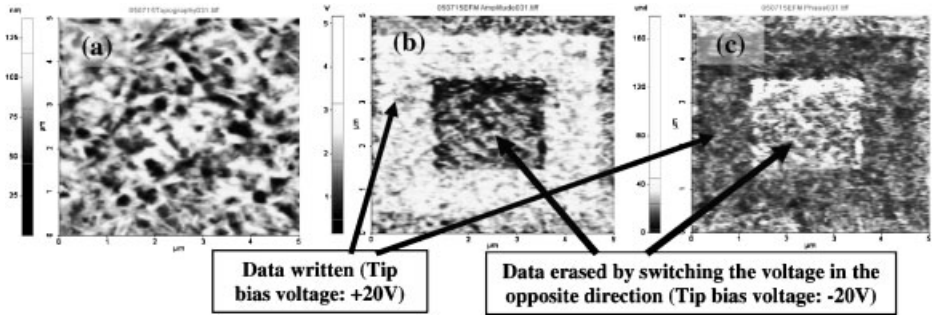

Figure 6.
(a) Topographic image after first poling the 200 nm thick P(VDF/TrFE) film on ITO. Piezoresponse (b) $A\cos\phi$ and (c) $A\cos\phi$ images observed after applying DC bias voltage.

edge-on crystalline grains. Figure 6(b) and (c) show the EFM amplitude and phase images observed in the initially poled area (data bit '1') and reversely poled area (data bit '0'). The data bit '1' was written with a dc bias voltage of +20V and the written data was erased with a dc bias voltage of −20V.

The image contrast of the polarized areas in the Figure 6(b) and (c) depends on the magnitude and direction of P_r after poling, since we used the ac modulating voltage of the constant V_{pp}. The formation of both domains is caused by the rotation and alignment of electric dipoles within P(VDF/TrFE) molecules in the direction of the applied electric field during poling process. After poling in a 4×4 μm^2 area, we applied a dc voltage with the opposite polarity in 2×2 μm^2 area inside the first poled area. As a result, the contrast in the amplitude and phase images was reversed, as shown in Figure 6(b) and (c). This phenomenon is a clear evidence of the polarization reversal, which is attributed to the 180° rotation of C-F dipoles in P(VDF/TrFE) along the molecular chains in accordance with the polarity of the applied dc bias. Since the poling direction is clearly discerned as shown in this figure, we find it feasible to apply piezoelectric ultrathin P(VDF/TrFE) films in SPM-based storage device of WMRM (Write-Many-Read-Many) ability by replacing PMMA film used in SPM-based storage device of WORM (Write-Once-Read-Many) ability.[6]

Conclusions

FTIR-GIRAS and AFM were used complementarily in analyzing surface crystalline morphology and chain orientation of ultrathin ferroelectric P(VDF/TrFE)(72/28) copolymer films prepared with varying thermal histories. For the as-cast (AC) and annealed (AN) samples, most of polymer chains were preferentially oriented along the substrate surface and edge-on lamellar crystals were formed predominantly. On the contrary, melt-crystallized samples (MQ and MSC) gave rise to preferential chain orientation along the normal to the surface plane and predominant face-on lamellar crystals. Thus the AN sample showed the largest remnant polarization and the smallest coercive field due to the easiest CF_2 dipole rotation by an external electric field, since the AN sample has preferential chain orientation along the conductive substrate surface with higher degree of crystallinity than in the AC sample. From these phenomena, we could find out that as-cast and then annealing at the temperature (ca. 120 °C) above Curie transition, but below melting transition temperature is the most suitable condition to fabricate the nonvolatile ferroelectric polymer memory device when P(VDF/TrFE) is used for the purpose. DC-EFM technique was successfully used to 'write and erase' the data bit on the ultrathin P(VDF/TrFE) film by applying a

dc bias voltage much larger than coercive voltage with different polarities. And the data bit state could be read by measuring the piezoelectric response of the cantilever with a conductive tip with a lock-in amplifier by applying an ac modulating voltage whose V_{pp} is much less than the coercive voltage.

Acknowledgements: This study was supported by ''the National Research Program for the 0.1 Terabit Non-volatile Memory Development sponsored by Korea Ministry of Commerce, Industry and Energy'' (Project No. M10424040007-04L2404-00713) and Korea Science and Engineering Foundation (KOSEF) through the SRC/ERC Program of MOST/KOSEF (R11-2005-065).

[1] S. R. Forrest, *Nature* **2004**, *428*, 911.
[2] H. Shin, J. H. Lee, K. Lee, W. K. Moon, J. U. Jeon, G. Lim, Y. Park, J. H. Park, K. H. Yoon, *IEEE Trans. Ultrasonics, Ferroelectrics Frequency Control* **2000**, *47*, 801.
[3] H. Shin, S. B. Hong, J. H. Moon, J. U. Jeon, *Ultramicroscopy* **2002**, *91*, 103.
[4] H. J. Mamin, B. D. Terris, L. S. Fan, R. C. Barrett, D. Rugar, *IBM J. Res. Develop.* **1995**, *39*, 681.
[5] S. Hosaka, A. Kikukawa, H. Koyanagi, T. Shintani, M. Miyamoto, K. Nakamura, K. Nakamura, K. Etoh, *anotechnology* **1997**, *8*, A58.
[6] H. J. Nam, S. Jang, Y. S. Kim, C. S. Lee, I. J. Cho, J. U. Bu, *J. Semicon. Technol. Sci.* **2005**, *5*, 24.
[7] P. Vettiger, J. Brugger, M. Despont, U. Drechsler, U. Drechsler, U. Durig, W. Haberle, M. Lutwyche, H. Rothuizen, R. Stutz, R. Widmer, G. Binnig, *Microelectron. Eng.* **1999**, *46*, 11.
[8] Q. M. Zhang, H. Xu, F. Fang, Z. Y. Cheng, F. Xia, *J. Appl. Phys.* **2001**, *89*, 2613.
[9] T. J. Reece, S. Ducharme, A. V. Sorokin, M. Poulsen, *Appl. Phys. Lett.* **2003**, *82*, 142.
[10] F. Xia, B. Razavi, H. Zu, Z. Y. Cheng, Q. M. Zhang, *J. Appl. Phys.* **2002**, *92*, 3111.
[11] K. Kobayashi, H. Masuda, H. Yamada, K. Matsushige, *Eur. Polym. J.* **2004**, *40*, 987.
[12] N. Tsutsumi, A. Ueyasu, W. Sakai, C. K. Chiang, *Thin Solid Films* **2005**, *483*, 340.
[13] I. L. Guy, J. Unsworth, *J. Appl. Phys.* **1987**, *61*, 5374.
[14] A. A. Prabu, J. S. Lee, K. J. Kim, H. S. Lee, *Vib. Spec.* **2006**, *41*, 1.
[15] X. Y. Jin, K. J. Kim, H. S. Lee, *Polymer* **2005**, *46*, 12410.
[16] Y. J. Park, S. J. Kang, C. M. Park, K. J. Kim, H. S. Lee, M. S. Lee, U. I. Chung, I. J. Park, *Appl. Phys. Lett.* **2006**, *88*, 242908.

